Full Length Article

Excitation process of Ce^{3+} and Eu^{2+} ions doped in $SrGa_2S_4$ crystals under the condition of multiplication of electronic excitations

Mamoru Kitaura [a,*], Senku Tanaka [b], Minoru Itoh [c], Akimasa Ohnishi [a], Hiroko Kominami [d], Kazuhiko Hara [d]

[a] Department of Physics, Faculty of Science, Yamagata University, Yamagata 990-8560, Japan
[b] Department of Electric and Electronic Engineering, Faculty of Science and Engineering, Kinki University, Higashiosaka 577-8502, Japan
[c] Department of Electrical and Electronic Engineering, Faculty of Engineering, Shinshu University, Nagano 380-8553, Japan
[d] Research Institutes of Electronics, Shizuoka University, Hamamatsu 432-8011, Japan

ABSTRACT

Excitation spectra for 5d–4f photoluminescence (PL) bands of Ce^{3+} and Eu^{2+} ions doped in $SrGa_2S_4$ crystals have been measured at room temperature in the energy region up to 25 eV. These spectra allow us to investigate the excitation process of luminescent ions under host excitation with vacuum ultraviolet (VUV) photons. A gentle increase in intensity is commonly observed at around 16.5 eV in the excitation spectra. Optical constant spectra were obtained from measurements of reflectivity and absorption edge spectra of undoped $SrGa_2S_4$ crystals. These data were compared with the results of a relativistic DV-Xα calculation, to clarify the electronic structure of $SrGa_2S_4$. Ultraviolet photoelectron spectroscopy (UPS) has been carried out under the excitation with photons in the 12–20 eV range. The detailed analysis of UPS spectra reveals that the multiplication of electronic excitations (MEEs) occurs above 16.5 eV. The excitation process of Ce^{3+} and Eu^{2+} ions is discussed together with the processes of MEEs.

© 2015 Elsevier B.V. All rights reserved.

1. Introduction

Multiplication of electronic excitations (MEEs) in wide-gap ionic crystals takes place when the energy of an excitation photon exceeds several times of their band-gap energies. The processes of MEEs have been investigated by photoluminescence (PL) and photoelectron spectroscopy with vacuum ultraviolet (VUV) photons [1–4]. The primary process of MEEs by VUV photons is explained on the basis of an inelastic scattering of hot photoelectrons with valence electrons. On the other hand, the excitation processes of luminescent ions doped in the wide-gap materials have also been studied in the VUV region [5–9]. Lushchick et al. [5] have measured VUV excitation spectra for Mn^{2+} intra-3d PL band of ZnS doped with Mn^{2+} ions of high-concentration, and observed a rapid increase in PL intensity at the photon energy lower than the threshold for MEEs in host ZnS. This phenomenon has been attributed to direct (elastic) impact excitation of hot photoelectrons with Mn^{2+} 3d electrons. This type of excitation has been found in VUV excitation spectra for Tl^+ 6p–6s PL bands of KCl and KBr doped with Tl^+ ions [4,7], and for Er^{3+} 5d–4f PL band of $LiYF_4$

doped with Er^{3+} ions [8]. In contrast, excitation spectra for Ag^+ 4s–3d PL band of NaCl doped with Ag^+ ions [9] and for Gd^{3+} intra-4f PL band of $Gd_3Al_2Ga_3O_{12}$ [10] did not show any evidence on such direct impact excitation. As mentioned here, the excitation processes of luminescent ions in the VUV region are sensitive to the electronic structures of host materials and luminescent ions, the concentration of luminescent ions and so on. In addition, these processes are expected to be complex, because they take place through a number of competing processes. Hence, they are still the subject of considerable discussion, and thus are worthwhile studying to find a collective view on these processes. The information would be useful in applications to luminescent devices in which hot conduction electrons play an important role for the excitation of luminescent ions.

Strontium thiogallate ($SrGa_2S_4$) activated using rare earth ions are known as a bright inorganic phosphor for solid-state lightening and information display [11,12]. The emission spectra exhibit prominent bands at 2.79 and 2.33 eV for Ce^{3+}- and Eu^{2+}-doped $SrGa_2S_4$, respectively. Since these bands are efficiently excited with photons in the absorption due to 4 f–5d transitions of Ce^{3+} and Eu^{2+} ions, they have been assigned to the 5d–4f transitions [13–18]. The onsets of Ce^{3+} and Eu^{2+} 4f–5d absorption locate at around 2.8 and 2.5 eV, respectively. Many experimental data on PL properties have been accumulated so far; however,

most of them concern the direct 4f–5d excitation, and there is few data obtained under photoexcitation in the fundamental absorption region of host $SrGa_2S_4$. Furthermore, fundamental optical properties and electronic structure of $SrGa_2S_4$ have not been investigated in detail. These data are of a great significance in understanding of relaxation of hot photoelectrons created under host excitation, and of the interaction of luminescent ions with them.

In the present study, we have measured excitation spectra for 5d–4f PL bands of Ce^{3+}- and Eu^{2+}-doped $SrGa_2S_4$ crystals, respectively, with use of synchrotron radiation. The reflectivity and absorption spectra of $SrGa_2S_4$ crystals were also measured to determine basic optical constant spectra by a Kramers–Kronig (KK) analysis and to correct the influence of reflection loss at the crystal surface on excitation spectra. The electronic structure calculation of $SrGa_2S_4$ was performed by a relativistic DV-Xα method. The energy level structure and partial density of states (PDOS) enable better understanding of optical spectra. Furthermore, ultraviolet photoelectron spectroscopy (UPS) spectra were measured at various excitation energies, to obtain the knowledge on the process of MEEs in $SrGa_2S_4$. The excitation processes of Ce^{3+} and Eu^{2+} ions by VUV photons are clarified from comparisons of experiment results and calculation. The relaxation processes of photoholes are also briefly discussed using a simplified energy band diagram.

2. Experiment

Crystals of undoped $SrGa_2S_4$, and Ce^{3+}- and Eu^{2+}-doped $SrGa_2S_4$ were grown by a chemical vapor transport technique using iodine as a transport agent [15]. Synthesized powders of undoped $SrGa_2S_4$, and Ce^{3+}- and Eu^{2+}-doped $SrGa_2S_4$ were inserted into quartz ampoules, which were sealed after evacuating in vacuum. The ampoules were placed in an electric furnace with two heating zone for two weeks. The temperatures of growth and source zones were kept at 900 and 750 °C, respectively. The average size of grown crystals was $2 \times 2 \times 0.1$ mm^3. The ab plane was used in our experiment. Excitation and reflectivity spectra were measured at the BL3B beamline of UVSOR in the Institute for Molecular Science (IMS). Synchrotron radiation (SR) was monochromatized through a 2.5-m normal incidence monochromator. The incident, reflected and transmitted photons were detected using a calibrated Si photodiode (IRD, XUV100) placed in the sample chamber. The intensities of reflected and transmitted photons were divided by that of the incident photon, in order to determine the reflectivity and absorption coefficient at various photon energies. PL was detected using the system consisting of two quartz lenses, a color filter, a grating monochromator, and a photomultiplier tube. Excitation spectra were corrected for the intensity distribution of the excitation light source and the reflection loss at the crystal surface.

UPS experiment was carried out at the BL8B beamline of UVSOR. $SrGa_2S_4$ thin-films were deposited on gold-coated quartz substrates heated at 200 °C using electron beam sources. The thickness was adjusted to be 50 nm using a quartz oscillator. As-deposited thin-films were annealed at 850 °C in H_2S+Ar gas mixture for 30 min, in order to supply deficient sulfur ions. The thin-films obtained are undoubtedly of polycrystalline, because substrates are made of silica glass. From the X-ray diffraction measurement, they were confirmed to be $SrGa_2S_4$. In UPS experiment, the surfaces of samples were cleaned in vacuum of 3×10^{-8} Pa with an Ar^+ ion gun. An appearance of the clean surface was judged from the peak energy and spectral shape of the Ga-3d peak. The energy distribution of photoelectrons emitted from the sample surface was analyzed using a hemi-spherical electron analyzer of 75 mm mean radius. The plane grating

monochromator (PGM) was used to obtain monochromatic excitation light. The intensity of the incident light was monitored using a gold mesh installed in front of the measurement chamber. UPS spectra were measured at room temperature. The spectral resolution of UPS spectra was 0.5 eV. The bias voltage of -15.0 V was applied to samples, in order to avoid the influence on a weak electric field generated around the sample holder and the analyzer. All the UPS spectra were divided by the photoelectric yield of the gold mesh. No significant effect of surface charging was observed.

3. Results

Fig. 1(a) shows the spectra of reflectivity (blue line) and absorption edge (red line) for an undoped $SrGa_2S_4$ crystal at room temperature. The fundamental absorption edge locates at around 4.1 eV. The reflectivity shown here is the absolute value obtained as follows. (i) The refractive index n below 4 eV is determined by the spectroscopic ellipsometry. (ii) The absolute reflectivity spectrum is calculated by substituting the values of n into the formula $R(E) = (n(E)-1)^2/(n(E)+1)^2$. (iii) The measured spectrum is connected to the calculated spectrum by multiplication with a constant factor. A weak exciton-like peak is observed at 4.72 eV. Assuming that the direct band-to-band transition occurs in the high-energy side of this peak, we roughly estimate the band-gap energy to be 4.8 eV. The most prominent peak appears at around 6.24 eV. As the photon energy is increased, the reflectivity is gradually decreased in the 15–20 eV range. Two weak peaks are seen at 21.7 and 22.7 eV.

Fig. 1(b) and (c) shows excitation spectra for 2.79 eV PL band of Ce^{3+}-doped $SrGa_2S_4$ and 2.33 eV PL band in Eu^{2+}-doped $SrGa_2S_4$, respectively. The concentrations of Ce^{3+} and Eu^{2+} ions were
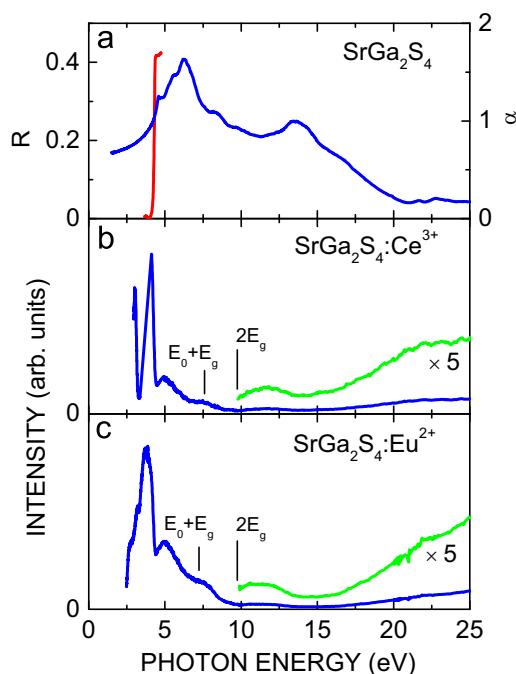
Fig. 1. (a): reflectivity (blue line) and absorption-edge (red line) spectra of an undoped $SrGa_2S_4$ crystal. (b) and (c): excitation spectra (blue line) for 5d–4f PL bands of Ce^{3+} and Eu^{2+} ions doped in $SrGa_2S_4$ crystals, respectively. The excitation spectra in the 10–25 eV range (green line) were magnified by a factor of 5. These spectra were obtained at room temperature. E_g and E_0 are the bad-gap energies and the onsets of the 4f–5d absorption of Ce^{3+} and Eu^{2+} ions in $SrGa_2S_4$, respectively. (For interpretation of the references to color in this figure legend, the reader is referred to the web version of this article.)

1.0 and 2.0 mol%, respectively. These data were measured at room temperature. In Fig. 1(b), the intensity of 2.79 eV band is high under photoexcitation in the energy region below 4.1 eV, the energy of which corresponds to the fundamental absorption edge. The intensity is drastically decreased with increasing photon energy, and is kept low under photoexcitation in the fundamental absorption region. A dip appears at 13.4 eV, where the reflectivity spectrum also exhibits a peak. These results suggest that non-radiative decay of electron–hole pairs occurs near the crystal surface under excitation with photons of high reflectivity. Magnifying the excitation spectrum in the 10–25 eV range, we notice a gentle increase in intensity above 16.5 eV. Except the energy region below 4.1 eV, the spectral feature mentioned here is almost the same as the excitation spectrum for 2.33 eV band of Eu^{2+}-doped $SrGa_2S_4$ (Fig. 1(c)).

We have obtained the spectra of optical constants from the reflectivity spectrum of Fig. 1(a) by the KK analysis. The KK analysis requires the reflectivity over the whole energy range from 0 to ∞. Since the actual reflectivity measurement is restricted to a finite energy range, the reflectivity was set to be constant below 1.5 eV, and was extrapolated using a function $R(E) = R(30 \text{ eV}) \cdot (30/E)^p$ above 30 eV, where p is an adjustable parameter. The parameter p was adjusted to be 2.57, so that the value of ε_2 is zero at the fundamental absorption edge. The spectra of the complex dielectric constant $\varepsilon = \varepsilon_1 + \varepsilon_2$, effective number of electrons per molecule N_{eff}, and electron energy loss function $-Im(1/\varepsilon)$ are shown in Fig. 2(a)–(c), respectively. The value of N_{eff} is given by the following equation [19]:

$$N_{eff} = \frac{2m}{N_m h^2 e^2} \int_0^E E' \epsilon_2(E') dE', \qquad (1)$$

where N_m is the number of molecules per unit volume, e and m are the charge and mass of electrons, and h is the Planck constant. In Fig. 2(a), the value of ε_1 is the highest at 4.53 eV, and is negative in
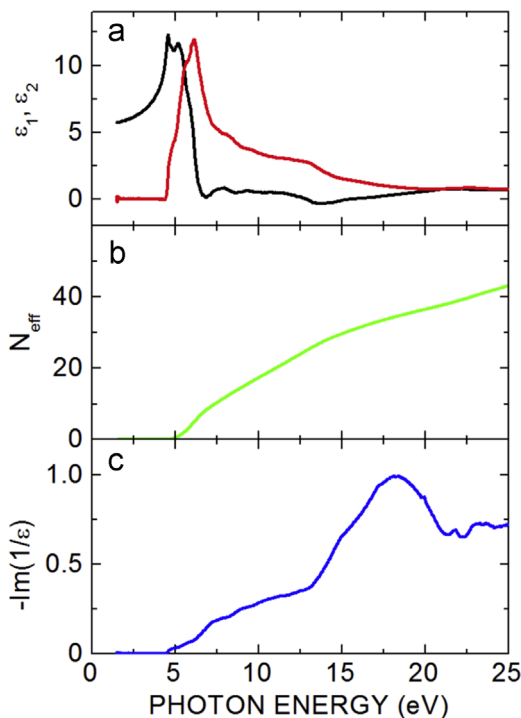
the 12.8–15.6 eV range. The value of ε_2 reaches the maximum at 6.1 eV. In Fig. 2(b), the value of N_{eff} is monotonically increased with photon energy. In Fig. 2(c), the $-Im(1/\varepsilon)$ spectrum exhibits a broad band around 18 eV.

In order to obtain information on relaxation processes of hot photoelectrons in host $SrGa_2S_4$, we measured UPS spectra of $SrGa_2S_4$ thin-films at room temperature under the excitation with 12.0–19.5 eV photons. The results are shown in Fig. 3. They mainly consist of two parts: high- and low-energy ones. As the photon energy is increased from 14 to 19 eV, high-energy part shifts to higher kinetic energy side, and is gradually weakened. In contrast, low-energy part stays at the kinetic energy smaller than 2.5 eV, and is slightly strengthened. The high-energy part is due to the photoelectron emission from the valence band. The low-energy part results not only from the photoelectron emission from the valence band, but also from the secondary electron emission. The secondary electron emission is regarded as an indication of MEEs in $SrGa_2S_4$.

The electron affinity χ is also one of the band parameters characterizing material properties. This value is determined from measurements of UPS spectra, and is calculated using the following equation [20],

$$\chi = h\nu - E_k^t - E_g, \qquad (2)$$

where $h\nu$ is the energy of exciting photons, and E_k^t is the highest energy threshold for the kinetic energy of photoelectrons. The difference between $h\nu$ and E_k^t, namely, ionization potential, is calculated to be 5.0 eV from Fig. 3. Considering the value of E_g to be 4.8 eV from the reflectivity spectrum of Fig. 1(a), the value of χ is estimated to be 0.2 eV in $SrGa_2S_4$.

The photon-energy dependence of the peak intensities of high- and low-energy parts in Fig. 3 is critical to clarify the secondary electron emission in the process of MEEs. However, it is not easy to determine the peak intensity of low-energy part, especially under excitation below 16 eV, because it strongly overlaps with the high-energy part which is dominant in UPS spectra of Fig. 3. Thus, the contribution of the high-energy part to the low-energy part has to

Fig. 2. (a): real part ε_1 (black line) and imaginary part ε_2 (red line) of the dielectric constant derived from the KK analysis. (b): the effective number of electrons per molecule N_{eff}. (c): electron energy loss function $-Im(1/\varepsilon)$. (For interpretation of the references to color in this figure legend, the reader is referred to the web version of this article.)
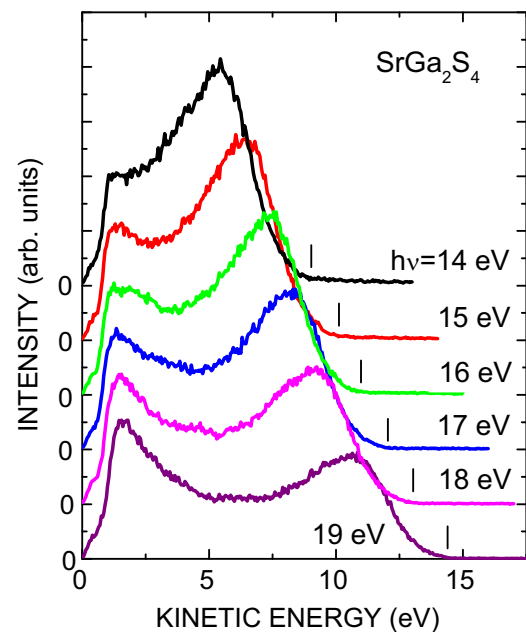
Fig. 3. Ultraviolet photoelectron spectroscopy (UPS) spectra of a $SrGa_2S_4$ thin-film on gold coated quartz substrate, measured at room temperature under excitation with VUV photons in the 14–19 eV range. The energy was referred to the top of the valence band. Vertical bars indicate the highest energy thresholds (E_k^t) for the kinetic energy of photoelectrons.
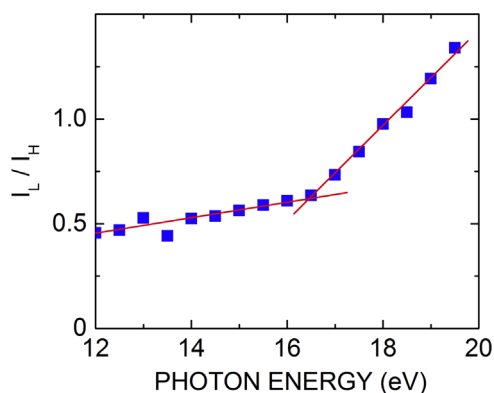
Fig. 4. Photon energy dependence of the intensity ratio of the high- and low-energy parts I_L/I_H, which were determined from the analysis of UPS spectra. The red line was drawn for eye guides.

Fig. 5. Energy level diagram and partial density of states (PDOS) per molecule calculated for the embedded $[Sr_9Ga_{12}S_{64}]^{74-}$ cluster. Solid and broken lines in the energy level diagram represent occupied and unoccupied states, respectively. The energy distribution curves of PDOS are shown for the atomic orbitals of Sr, Ga, and S. The top of the VB was taken as zero energy.

be evaluated from Fig. 3. To do so, the peak intensity ratio of the high- and low-energy parts I_L/I_H was obtained in the present study. Fig. 4 represents the photon-energy dependence of I_L/I_H. We can recognize that the value of I_L/I_H is almost constant in the low-energy region, but exhibits a remarkable increase in the region above 16.5 eV.

4. Electronic structure by DV-Xα calculation

No electronic structure calculation is available for $SrGa_2S_4$. We have performed a molecular orbital (MO) calculation on this crystal by a relativistic DV-Xα method. The calculation procedures have been described in literatures [21,22]. This method is one of cluster approaches which are beneficial not only to the analysis of electronic structures of crystalline solids but also to the prediction of various material properties. The crystal structure of $SrGa_2S_4$ is orthorhombic, and the space group is Fddd [23]. In this calculation, a $[Sr_9Ga_{12}S_{64}]^{74-}$ molecular ion was picked up from the $SrGa_2S_4$ crystal lattice, and was used as a model cluster. A Sr^{2+} ion locates at the center of this cluster. The point symmetry is D_2. The basic functions used were 1s–5p orbitals for Sr, 1s–4p for Ga, and 1s–3p for S. The charge of the model cluster was canceled out by considering the Madelung potential generated by point charges outside it.

The energy level diagram and partial density of states (PDOS) for the $[Sr_9Ga_{12}S_{64}]^{74-}$ cluster are shown in Fig. 5. The band-gap energy E_g and valence band width ΔE_V were determined to be 4.58 and 6.56 eV, respectively. Both are supposed to be reasonable, compared to the absorption edge spectrum (Fig. 1(a)) and UPS spectra (Fig. 3), respectively. Seeing PDOS of each MO level, we notice that the valence band is dominated by the S-3p state with Ga-4s and -4p character. The bottom of the conduction band is made up of Ga-4s and S-3p states. The PDOS of the Sr-4d state locating at the higher position is large, compared with those of Ga-4s and S-3p states. Core bands of Sr-4p, Ga-3d, and S-3s are seen below the valence band. This feature is consistent with the literature on X-ray photoelectron spectroscopy (XPS) [24]. However, the calculated binding energies for core levels are apparently underestimated, compared to the XPS peaks. This is because orbital relaxation induced by the creation of core holes is not taken into consideration in our calculation.

5. Discussion

We first discuss optical properties of $SrGa_2S_4$ by referring to the electronic structure. In Fig. 1(a), a weak peak is observed at 4.72 eV, which is naturally assigned to the electronic transition from the top of the valence band of S-3p state to the bottom of the conduction band of Ga-4s state. This peak would be connected to the creation of excitons, but it is not so sharp compared to the lowest absorption peaks in halide crystals. We suppose that the effect of the electron–hole interaction, i.e., exciton effect, is weak in $SrGa_2S_4$. The excitons in this crystal may be thermally decomposed into an electron–hole pair at room temperature, because of its small binding energy ($\sim$0.08 eV). The most intense peak locates at around 6.24 eV. As seen in Fig. 5, the PDOS of S-3p and Sr-4d peaks are highest among valence and conduction band peaks, respectively. It is thus reasonable to assign the 6.24 eV peak to the interband transition from the valence band of S-3p state to the lower conduction band of Sr-4d state. The broad peak around 13 eV is likely assigned to the interband transition from the valence band to the higher conduction band of Sr-5p state. Two weak peaks appear at 21.72 and 22.74 eV, being nearly close to the sum of the band-gap energy and the Ga-3d core level energy. The energy separation between them is larger than the Ga-3d spin–orbit splitting energy ($\sim$0.4 eV). From these facts, the two peaks would be due to the superposition of Ga-3d core peaks at critical points [25].

In Fig. 2(b), the value of N_{eff} is 24 at 12.5 eV. This value is the same as the number of valence electrons per $SrGa_2S_4$ molecule, calculated from the sum of 3p electrons of four S^{2-} ions. From Fig. 5, the sum of E_g and ΔE_V is estimated to be 11.14 eV. The photon of 12.5 eV has the energy enough to put up an electron from the bottom of the valence band to the lower conduction band. All the valence electrons are thus exhausted under photo-excitation with photons above 12.5 eV.

As seen in Fig. 2(a), the value of ε_1 is increased in the 13.5–20 eV range, while the value of ε_2 is decreased. This feature suggests that excited electrons of $SrGa_2S_4$ respond as if they are free electrons. Optical excitation in this range carries electrons to the S-3s and -3p states in the conduction band. The resulting conduction electrons will cause collective oscillations due to the effect of the electric field of photons, leading to the formation of bulk plasmons. The formation energy E_p of a bulk plasmon is generally
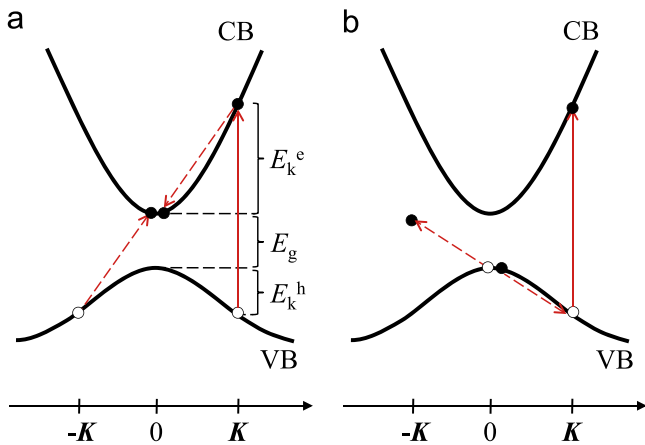
Fig. 6. Schematic model on relaxation processes of a hot photoelectron (a) and a photohole (b) in a simplified energy band diagram. The energies of band-gap E_g and valence band width ΔE_V were based on the calculated energy level structure of Fig. 5. Solid arrows indicate photoexcitation from the valence band (VB) to the conduction band (CB). Broken arrows depict nonradiative Auger transitions.

given by the following equation [19];

$$E_p = \sqrt{\frac{N_e h^2 e^2}{\pi m}}, \tag{3}$$

where N_e is the number of conduction electrons per unit volume. From Eq. (3), we obtain $E_p = 16.4$ eV. The value of E_p is within the prominent peak at 18 eV in Fig. 2(c). It is, therefore, likely to connect the 18 eV peak to the bulk plasmon formation.

Let us discuss the process of MEEs in SrGa$_2$S$_4$ caused by VUV excitation. In Fig. 4, one can see a remarkable increase of I_L/I_H at around 16.5 eV. Optical excitation at around 16.5 eV leads to the electronic transitions from the valence band, which enables to create hot photoelectrons with the kinetic energies larger than E_g. In this case, the hot photoelectrons can kick up valence electrons to the conduction band through inelastic scattering. Thus, the increase of I_L/I_H is interpreted as an indication of MEEs, due to inelastic scattering of hot photoelectrons with valence electrons.

The threshold E_{th} for MEEs is estimated to be 16.5 eV, which is more than twice of E_g. This result is qualitatively explained by using a simplified energy band diagram with direct band-gap. Fig. 6(a) and (b) shows a schematic model on relaxation processes of a hot photoelectron and a photohole, respectively. The energies of E_g and ΔE_V are referred to the calculated energy level structure of Fig. 5. When a photon with the energy of $h\nu$ excites a valence electron at the wave vector K, a hot photoelectron and a photohole are both created at the wave vector K. The former has the kinetic energy E_k^e, and the latter has the kinetic energy E_k^h. When the momentum-conservation law is satisfied in the process of impact excitation, hot photoelectron with K would kick up a valence electron with $-K$ to the conduction band bottom at $K=0$ (Fig. 6 (a)). The valence hole thus created at $-K$ has the same kinetic energy as the photohole at K. Since this impact process completes in a very short time, hot photoelectrons do not have any time to interact with phonons. Furthermore, the energy-conservation law requires $E_k^e = E_k^h + E_g$. Since the photon energy $h\nu$ required to cause MEEs is given by the sum of E_k^e, E_k^h and E_g, we get $E_{th} = 2E_g + 2E_k^h$. It is, therefore, reasonable to expect that the value of E_{th} exceeds the twice of E_g. As described above, the simplified energy band diagram is well adopted in a phenomenological explanation of MEEs in SrGa$_2$S$_4$; however, it has applicable limits, especially for the quantitative analysis of E_{th}. In that case, more advanced theoretical approach based on the multiple-parabolic-branch band model [26] would be worthy of note.

The condition $\Delta E_V > E_g$ may imply the possibility that photoholes also participate in the process of MEEs [27]. As show in Fig. 6 (b), the hot photohole with $-K$ has a chance to kick up a $K=0$ valence electron situating at the top of the valence band. In such an excitation process, however, there is no final state for the $K=0$ valence electron. Since the momentum-conservation law is not satisfied in the relaxation process of photoholes, they cannot relax quickly through the Auger process. Consequently, photoholes will lose their kinetic energies through the interaction with phonons, to relax to the valence band top. The energy loss resulting from relaxation of photoholes, so-called hole energy losses, has been observed in wide-gap materials with the condition of $\Delta E_V > E_g$ [28]. Details of hole energy losses still remain invisible. Further experimental and theoretical investigations are desired to solve this fundamental problem.

Finally, we consider the excitation process of Ce^{3+} and Eu^{2+} ions by VUV photons. As shown in Fig. 1(b) and (c), intensities of 5d–4f PL bands of Ce^{3+} and Eu^{2+} ions are remarkably low in the fundamental absorption region, compared to those in the 4f–5d absorption region. This fact is probably due to the difference in penetration depth of excitation photons. UV–VUV photons cannot penetrate toward the inside of crystal, because the absorption coefficient is much high in the fundamental absorption region. If created electron–hole (e–h) pairs cannot migrate in a long distance, very small amounts of Ce^{3+} and Eu^{2+} ions will be excited near the surface layers, which leads to the low efficiency of host-sensitized Ce^{3+} and Eu^{2+} PL.

A gentle increase in intensity is found around 16.5 eV in the excitation spectra of Fig. 1(b) and (c). This is apparently connected to the MEEs in SrGa$_2$S$_4$, because it agrees with the threshold energy for MEEs. The intensities at 22 eV are two times larger than those at 12 eV where a photon creates one e–h pair. This may indicate that two e–h pairs are formed after relaxation of hot photoelectrons, resulting in the twofold increase in intensity, and is compatible with our assignment that the process of MEEs is caused by the inelastic scattering of hot photoelectrons with valence electrons.

It is noted that the excitation spectra for 5d–4f PL bands of Ce^{3+} and Eu^{2+} ions are almost the same with each other. This suggests that Ce^{3+} and Eu^{2+} ions are not directly excited by hot photoelectrons, in contrast with s^2 type metal ions in alkali halides [4,5] and Er^{3+} ion in LiYF$_4$ [8]. Fig. 1(b) and (c) shows $E_{th} > E_0 + E_g$, where E_0 is the lowest threshold energies for 4f–5d absorption of Ce^{3+} and Eu^{2+} ions. This fact strongly supports that no direct excitation of 4f electrons in Ce^{3+} and Eu^{2+} ions by hot photoelectrons occurs in SrGa$_2$S$_4$. Furthermore, no intrinsic PL band is found in SrGa$_2$S$_4$, indicating that the nonradiative resonant energy transfer of Dexter type is impossible for Ce^{3+} and Eu^{2+} PL bands [29]. We believe that Ce^{3+} and Eu^{2+} ions will be converted to Ce^{4+} and Eu^{3+} ions, respectively, by capturing valence holes created under the MEE process. The resulting Ce^{4+} and Eu^{3+} ions form the excited states of Ce^{3+} and Eu^{2+} ions through the recombination with conduction electrons. The excited 5d states of Ce^{3+} and Eu^{2+} ions relax to the ground states, giving rise to 5d–4f PL bands in these ions.

6. Summary

The excitation processes of Ce^{3+} and Eu^{2+} ions doped in SrGa$_2$S$_4$ crystals have been investigated in the energy region up to 25 eV through the measurements of excitation spectra for 5d–4f PL bands. A gentle increase in intensity was commonly observed at around 16.5 eV in both excitation spectra. This feature was attributed to the MEEs of SrGa$_2$S$_4$. No direct excitation process of Ce^{3+} and Eu^{2+} ions by hot photoelectrons could be seen. The

electronic structure of $SrGa_2S_4$ has also been studied through the measurement of the reflectivity spectrum and the theoretical calculation by a relativistic DV-Xα method. It was clarified that the valence band is mainly of S-2p states, and the conduction band is composed of Ga-3s and Sr-4d mixed states. The band-gap energy was calculated to be 4.58 eV, being narrower than the valence band by 1.98 eV. The process of MEEs has been investigated by measuring UPS spectra. It was suggested that the MEEs is caused by the inelastic scattering of hot photoelectrons with valence electrons.

If the condition $\Delta E_V > E_g$ is really satisfied in $SrGa_2S_4$, it is expected that photoholes also participate in the process of MEEs. The present experiment, however, did not provide positive evidence for this expectation. The existence of photoholes in the process of MEEs is very interesting from the viewpoint of fundamentals in solid-state physics and material science. The relaxation of hot photocarriers created by VUV radiation should be deeply investigated using time-resolved UPS technique combined with SR and femtosecond laser.

Acknowledgments

References

[1] Ch. Lushchik, E. Feldbach, A. Frorip, M. Kirm, A. Lushchik, A. Maaroos, I. Martinson, J. Phys.: Condens. Matter 6 (1994) 11177.
[2] A. Lushchik, E. Feldbach, Ch. Lushchik, M. Kirm, I. Martinson, Phys. Rev. B 50 (1994) 6500.
[3] A. Lushchik, E. Feldbach, R. Kink, Ch. Lushchik, M. Kirm, I. Martinson, Phys. Rev. B 53 (1996) 5379.
[4] M. Kitaura, M. Itoh, H. Nakagawa, M. Fujita, J. Phys. Soc. Jpn. 72 (2003) 730.
[5] Ch. Lushchik, E.R. Ilmas, I. Savikhina, in: Proceedings of the International Conderence on Luminescence, Budapest, 99, 1966.
[6] M. Kirm, E. Feldbach, T. Karner, A. Lushchik, Ch. Lushchik, A. Maaroos, V. Nagirnyi, I. Martinson, Nucl. Instrum. Methods Phys. Res. B 141 (1998) 431.
[7] E. Feldbach, M. Kamada, M. Kirm, A. Lushchik, Ch. Lushchik, I. Martinson, Phys. Rev. B 56 (1997) 13908.
[8] V.N. Makhov, N.M. Khaidukov, N. Yu Kirikova, M. Kirm, J.C. Krupa, T.V. Ouvarova, G. Zimmerer, J. Lumin. 87–89 (2000) 1005.
[9] E. Feldbach, M. Kirm, A. Lushchik, Ch. Lushchik, I. Martinson, J. Phys.: Condens. Matter 12 (2000) 1991.
[10] K. Fukui, R. Ikematsu, Y. Imoto, M. Kitaura, K. Nakagawa, T. Ejima, E. Nakamura, M. Sakai, M. Hasumoto, S. Kimura, J. Synchrotron Rad. 21 (2014) 452.
[11] K. Tanaka, Y. Inoue, S. Okamoto, K. Kobayashi, J. Cryst. Growth 150 (1995) 1211.
[12] I. RonotLimousin, A. Garcia, C. Fouassier, C. Barthou, P. Benalloul, J. Benot, J. Electrochem. Soc. 144 (1997) 687.
[13] C. Chartier, C. Barthou, P. Benalloul, M. Frigerio, Electrochem. Solid-State Lett. 9 (2006) G53.
[14] K. Tanaka, T. Ohgoshi, K. Kimura, H. Yamamoto, K. Shinagawa, K. Sato, Jpn. J. Appl. Phys. 34 (1995) L1651.
[15] A. Kato, M. Yamazaki, H. Najafov, K. Iwai, A. Bayramov, C. Hidaka, T. Takizawa, S. Iida, J. Phys. Chem. Solids 64 (2003) 1511.
[16] C. Hidaka, K. Miura, S. Oikawa, T. Takizawa, Phys. Status Solid A 203 (2006) 2718.
[17] M. Nagata, S. Okamoto, K. Tanaka, T. Sakai, A. Tamaki, Phys. Status Solidi A 206 (2009) 2613.
[18] M. Nagata, S. Okamoto, K. Tanaka, T. Sakai, H. Kawasaki, A. Tamaki, J. Lumin. 130 (2010) 2040.
[19] H.R. Philipp, E. Ehrenreich, Phys. Rev. 131 (2016) 1963.
[20] R.T. Poole, J.G. Jenkin, J. Liesegang, R.C.G. Leckey, Phy. Rev. B 11 (1975) 5179.
[21] H. Adachi, M. Tsukada, C. Satoko, J. Phys. Soc. Jpn. 45 (1978) 875.
[22] K. Ogasawara, T. Iwata, Y. Koyama, T. Ishii, I. Tanaka, H. Adachi, Phys. Rev. B 64 (2001) 115413.
[23] T.E. Peter, J. Baglio, J. Electrochem. Soc. 119 (1972) 230.
[24] J.F. Moulder, W.F. Stickle, P.E. Solo, K.D. Bomben, Handbook of x-ray photo-electron spectroscopy, Perkin-Elmer Cooperation, Eden, Prairie, MN, 1992.
[25] C.G. Olson, D.W. Lynch, A. Zehe, Phys. Rev. B 24 (1981) 4629.
[26] A.N. Vasil'ev, Y. Fang, V.V. Mikhailin, Phys. Rev. B 60 (1999) 5340.
[27] R. Kink, T. Avarmaa, V. Kisand, A. Lohmus, I. Kink, I. Martinson, J. Phys.: Condens. Matter 10 (1998) 639.
[28] A. Lushchik, M. Kirm, C. Lushchik, I. Martinson, V. Nagirnyi, F. Savikhin, E. Vasil'chenko, Nucl. Instrum. Methods A 308 (1991) 178.
[29] D.L. Dexter, J. Chem. Phys. 21 (1953) 836.